PHYSICAL REVIEW E VOLUME 50, NUMBER 5 NOVEMBER 1994

Multifractality of large turbulent fluctuations and the topology of strange attractors

A. Bershadskii[1] and A. Mikishev[2]
[1]*P.O.Box 39953, Ramat-Aviv 61398, Tel-Aviv, Israel*
[2]*School of Mathematical Sciences, Tel Aviv University, Tel Aviv 69978, Israel*
(Received 21 September 1993; revised manuscript received 25 March 1994)

The connection between the local self-generation of turbulence by the Zaslavsky-Rachko scenario (Zh. Eksp. Teor. Fiz. **76**, 2052 (1979) [Sov. Phys. JETP **49**, 1039 (1979)]) and the multifractality of turbulent energy is investigated. The effect of the topological singularities of the Zaslavsky attractor on the multifractal asymptotic is shown. The calculated value of the asymptotic generalized dimension is in good agreement with the experimental data. The model has also turned out to be applicable to passive scalar dissipation fields and to the quantitative description of turbulent diffusion in a stable stratified liquid.

PACS number(s): 47.27.−i

I. INTRODUCTION

It is known that the internal intermittency of turbulent flow leads to the existence of subregions with self-generation of turbulence in liquid. In these subregions quasilaminar motion becomes unstable and goes to chaos by one or another scenario. The properties of such a chaos depend on the type of scenario. This phenomenon is one of the sources of multifractal behavior of turbulence. Figure 1 plots the energy of turbulent velocity fluctuations taken from a grid-flow experiment [1, 2]. In this figure an abrupt blip can be seen. If this blip is the result of instability of the quasilaminar motion inside the subregions, then the Landau approach can be used to describe the collapse of the stable limit cycle upon turbulence generation [3]. The idea of Landau consists in the description of turbulence near the critical Reynolds number Re_c (here we speak of local Reynolds number), taking into account the most unstable mode with the complex frequency $\omega = \omega_1 + i\alpha_1/2$ ($\omega_1 \gg \alpha_1$) such that $\alpha_1 = 0$ if $\mathrm{Re}=\mathrm{Re}_c$. The fluctuations of the velocity field are decomposed as

$$\mathbf{u} = A(t)\mathbf{g}(\mathbf{r}, t), \tag{1}$$

with amplitude

$$A(t) \sim e^{\frac{\alpha_1}{2}t - i\omega_1 t}. \tag{2}$$

When $\alpha_1 > 0$, Eq. (2) is valid only for small values of t. To analyze the nonlinear stability problem, Landau proposed the following amplitude equation:

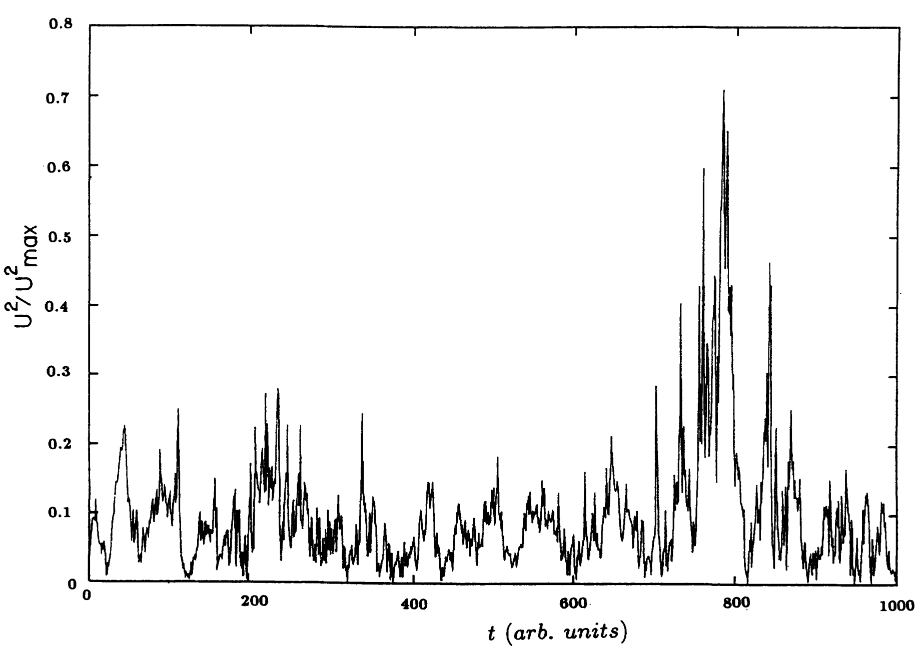

FIG. 1. Energy fluctuations in grid flow [1, 2].

1063-651X/94/50(5)/3723(7)/$06.00

$$\frac{d|A|^2}{dt} = \sum_{n=1}^{\infty} \alpha_n |A|^{2n} \tag{3}$$

under the assumption that the average over the time intervals smaller than α_1^{-1} and larger than ω_1^{-1} was taken. The simplest nonlinear approach, for small $|A|$, gives us

$$\frac{d|A|^2}{dt} = \alpha_1|A|^2 + \alpha_2|A|^4 , \tag{4}$$

with the nontrivial result for the asymptotic amplitude $(t \to \infty)$

$$|A|^2 \to -\alpha_1/\alpha_2. \tag{5}$$

Here $\alpha_1 > 0$ and $\alpha_2 < 0$ (supercritical case).

We investigate the local instability in stochastic media. Let us rewrite the amplitude equations as

$$\dot{A} = \{\cdots\} + f(t) \ , \quad \dot{A}^* = \{\cdots\}^* + f^*(t),$$

where $\{\cdots\}$ denotes the dynamic terms, $f(t)$ the external stochastic force from the turbulent environment, and $*$ defines the complex conjugation. If the correlation radius of external forces is smaller than typical times of the dynamical problem, then we can assume (in the first approximation) that $f(t)$ and $f^*(t)$ are Gaussian random functions with the mean value equal to zero:

$$\langle f(t) f^*(t')\rangle = 2\sigma_0^2 \delta(t-t').$$

Denote probability density for $I = |A|^2$ as

$$P_t(I) = \langle \delta(|A|^2 - I)\rangle.$$

Then after averaging over the times of order ω_1^{-1} and taking into account Eq. (4), we obtain the following Fokker-Planck equation for P_t:

$$\frac{\partial P_t(I)}{\partial t} = -\frac{\partial}{\partial I}\{(\alpha_1 I + \alpha_2 I^2)P_t(I)\} + 2\sigma_0^2 \frac{\partial}{\partial I}\left\{I\frac{\partial P_t}{\partial I}\right\}. \tag{6}$$

The stationary solution of (6) has the form

$$P_\infty(I) \sim \exp\left\{\frac{1}{2\sigma_0^2}\left(\alpha_1 I + \frac{\alpha_2}{2}I^2\right)\right\}\Theta(I), \tag{7}$$

where $\Theta(I)$ is the Heaviside function.

Maxima of $P_\infty(I)$ correspond to the local stable states and minima to the local unstable states (see [4, 5]). Figure 2 shows schematic dependence of P_∞ on I for $\alpha_1 > 0$ and $\alpha_2 < 0$. The initial state, $I = 0$, is statistically unstable and the state $I_0 = -\alpha_1/\alpha_2$ is stable [cf. with dynamical result (5)].

However, the short approximation (4) [or (6)] is not suitable for the investigation of high energy blips. Then the principal question is how many terms in (3) should we take into account to describe the large energy blip.

II. TOPOLOGY OF ZASLAVSKY STRANGE ATTRACTOR AND ORDER OF AMPLITUDE EQUATION

Paper [6] deals with a general model of the appearance of the strange attractor (Zaslavsky attractor) upon the collapse of the stable limit cycle. The authors of [6] introduced into the Landau amplitude equation for the supercritical limit cycle the interaction term that describes the interaction between modes along the entire spectrum:

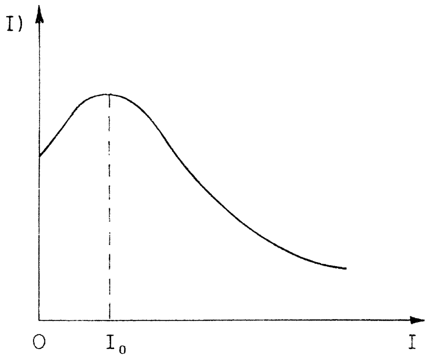

FIG. 2. Schematic sketch of $P_\infty(I)$ for supercritical Hopf bifurcation.

$$\dot{A} = \left(\frac{\alpha_1}{2} - i\omega_1\right) A + \alpha_2|A|^2 A + \sum_k V_{kk_0} a_k a_{k-k_0}. \tag{8}$$

Here the interaction matrix elements V_{kk_0} are determined directly from the original equations of motion. The wave number k_0 corresponds to the mode I_0. Then the equation for $I = |A|^2$ can be written as

$$\dot{I} = 2\alpha_2 I_0(I - I_0) + 2\Re\left\{A^* \sum_k V_{kk_0} a_k a_{k-k_0}\right\}, \tag{9}$$

where $I_0 = |A_0|^2 = -\alpha_1/\alpha_2$ is the original Landau cycle (see Introduction). The interaction matrix elements are approximated in [6] as

$$\sum_{k>k_0} V_{kk_0} a_k a_{k-k_0} \sim \sum_{n=-\infty}^{\infty} \delta(t - nT), \tag{10}$$

where the quantity T has the meaning

$$\frac{2\pi}{T} \sim \frac{d\omega}{dk} \triangle k$$

($\triangle k$ is the characteristic distance between neighboring wave numbers of the excited modes a_k). Let $A = |A|e^{i\theta}$. Substituting (10) into (9) we obtain the following system:

$$\dot{I} = -\gamma(I - I_0) + gq(I_0, \theta) \sum_{n=-\infty}^{\infty} \delta(t - nT), \tag{11}$$

$$\dot{\theta} = \omega(I), \tag{12}$$

where $q(I_0, \theta) = I_0 \cos\theta, \omega(I) = \omega_0 + \alpha\omega_0(I - I_0)/I$, and g and α are dimensionless parameters. Introducing new dimensionless quantities

$$y = (I - I_0)/I_0, \qquad x = \theta/(2\pi),$$

we obtain the following mapping:

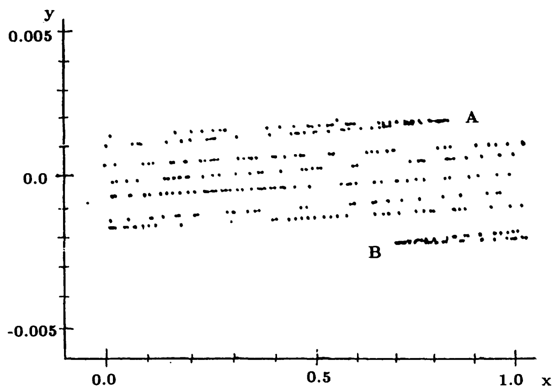

FIG. 3. Zaslavsky strange attractor for $\epsilon = 0.3$, $\alpha = 0.3$, $K = 9$, and $\Gamma = 5$.

$$y_{n+1} = e^{-\Gamma}(y_n + \epsilon \cos 2\pi x_n), \tag{13}$$

$$x_{n+1} = \left\{ x_n + \frac{1}{2\pi}\Omega(1 + \mu y_n) + \frac{1}{2\pi} K\mu \cos 2\pi x_n \right\}. \tag{14}$$

Here the brackets $\{\}$ denote the fractional part of the argument, $\Omega = \omega_0 T, \Gamma = \gamma T, K = \epsilon\alpha\Omega, \mu = (1 - e^{-\Gamma})/\Gamma$. Absence of dissipation corresponds to $\Gamma = 0$:

$$y_{n+1} = y_n + \epsilon \cos 2\pi x_n, \tag{15}$$

$$x_{n+1} = \left\{ x_n + \frac{1}{2\pi}\Omega(1 + y_n) + \frac{1}{2\pi} K \cos 2\pi x_n \right\}, \tag{16}$$

which is the basic model for the stochasticity of Hamiltonian systems.

In [6, 7], it is shown that, for the system (13) and (14), the strange attractor occurs in the case of strong dissipation ($1 < \Gamma < K$). Figure 3 shows a typical strange attractor in the phase plane for the system. For any initial condition the point of a trajectory lands after some time on the structure depicted in Fig. 3. Numerical analysis gives the existence of a stationary distribution function $\rho(x, y)$ in the strange attractor [6, 8, 9]. The distribution function has two sharp maxima in the neighborhood of points A and B (see Fig. 4 adapted from [6]). After the averaging over the phases and smoothing over small oscillations of $\rho(x, y)$, function $P_\infty(I)$ can schematically be depicted as in Fig. 5. Here I_- corresponds to the sharp maximum of $\rho(x, y)$ near point B, while I_+ corresponds to the sharp maximum of $\rho(x, y)$ near point A.

The existence of these two maxima is caused by the topology of the Zaslavsky strange attractor (in the case of strong dissipation). We can see from Figs. 3 and 4 that the attractor consists of two types of strips differing in their slopes. These strips have the fractal structure (see for example [10, 11]). In the vicinities of A and B, these strips interact by the appearance of bridges be-

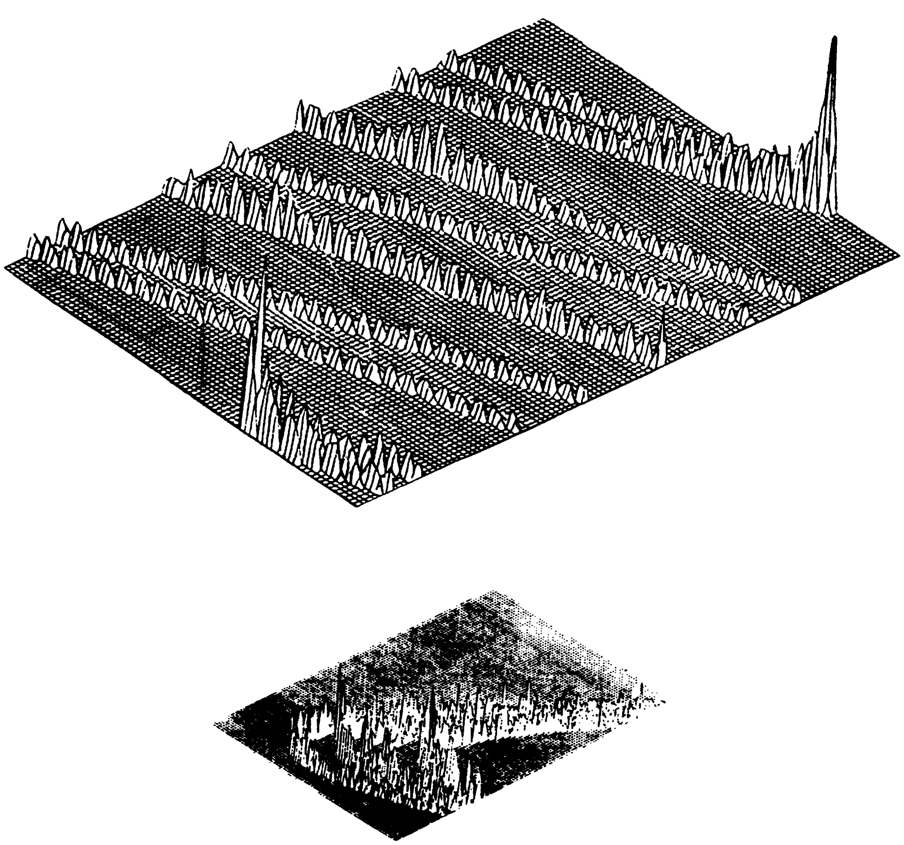

FIG. 4. Distribution function $\rho(x, y)$ on the strange attractor depicted in Fig. 3 [on bottom: the subdivision of the $\rho(x, y)$ in the vicinity of point B].

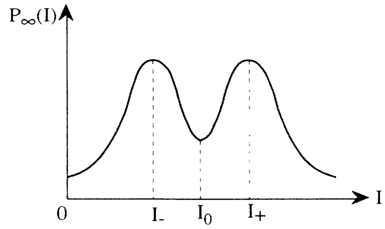

FIG. 5. Schematic sketch of $P_\infty(I)$ for averaging over the phases and smoothing distribution function $\rho(x,y)$.

tween them. At the bottom of Fig. 4, the subdivision of the distribution function in the vicinity of point B is shown. The existence of these bridges helps us to understand the nature of the sharp maxima. Each point on the strange attractor has its initial-data zone (IDZ) on the phase plane. The value of probability density at a fixed attracting point is determined by the area of its IDZ. The distribution of IDZ over these points has a short-range order on the strip, whereas on the bridge, the order is changed to the long-range one. This leads to the formation of sharp maxima of the probability density function on the bridges. Thus, if the intersection of strips occurs only in boundary points A and B [12], then the averaging over the phases and smoothing function $P_\infty(I)$ will look as in the schematic sketch in Fig. 5. This type of dependence of P_∞ on I corresponds to the following dynamical prototype (see Introduction):

$$\frac{d|A|^2}{dt} = \sum_{n=1}^{4} \alpha_n |A|^{2n}, \tag{17}$$

where the upper limit of summation, 4, is determined by the presence of two maxima in Fig. 5 [i.e., by topology of a strong dissipative ($\Gamma > 1$) Zaslavsky strange attractor].

III. ORDER OF AMPLITUDE EQUATION AND DIMENSION OF GOVERNING PARAMETER

Local equilibrium states of the dynamical system (17) are determined from the condition that the right side of the equation is equal to zero (i.e., $d|A|^2/dt \to 0$ in the vicinity of equilibrium). In our approach, see Introduction, the term $d|A|^2/dt$ plays the role of Kolmogorov parameter $\bar{\epsilon} = \langle \frac{1}{2} |\frac{d\mathbf{u}^2}{dt}| \rangle$ [13]. Thus, in the vicinity of the local (dynamic) equilibrium, the Kolmogorov approach does not work ($\bar{\epsilon} \sim d|A|^2/dt \to 0$). Then what kind of parameter governs our equilibrium states? If we suppose that in (17) parameter α_4 tends to zero, then the local equilibria are broken. $\bar{\epsilon}$ governs the balance between vortex stretching and viscous dissipation in the real space, while dynamical parameter α_4 governs the balance between stretching of the trajectories and effective diffusion in the phase space of the Zaslavsky attractor. As in the Kolmogorov approach (where from dimensional arguments we obtain the energetic spectrum $E \sim \bar{\epsilon}^{2/3} k^{-5/3}$), in the localized case we estimate scaling of the large energy blip as

$$\int_v \mathbf{u}^2 dv \sim \alpha_4^{-2/5} r^{13/5}, \tag{18}$$

where r is the spatial scale of the energy blip (see Introduction and [14]). The dimension of α_4 is defined by Eq. (17): $\alpha_4 \sim [T]^5 [L]^{-6}$.

The experimental checking of (18) can be done by the method of multifractal asymptotics [14–16]. Let us divide the fluid volume of size L into cells of size r and define the q moment of the field $\mathbf{u}^2$ as

$$\langle (\mathbf{u}^2)_r^q \rangle = \frac{\sum_{i=1}^{N} (\frac{1}{r^d} \int_{v_i} \mathbf{u}^2 dv)^q}{(L/r)^d}, \tag{19}$$

where q is a real number (order of moment), i is a number of cell, and d is topological dimension of the space. The multifractal hypothesis can be formulated as

$$\langle (\mathbf{u}^2)_r^q \rangle \sim r^{-\mu_q}, \tag{20}$$

with the intermittency exponent μ_q expressed versus generalized dimension D_q [16],

$$\mu_q = (d - D_q)(q - 1). \tag{21}$$

In paper [15] it is shown that

$$\max_i \int_{v_i} \mathbf{u}^2 dv \sim r^{D_\infty}. \tag{22}$$

If the experimentally determined μ_q leads to linear asymptotic, then the slope of the asymptotic is equal to $(d - D_\infty)$ [2, 14, 15]. Figure 6 shows μ_q obtained from the experimental data for grid flow ($\mathrm{Re}_\lambda = 70$), boundary layer flow ($\mathrm{Re}_\lambda = 290$), and jet flow ($\mathrm{Re}_\lambda = 880$) [1, 2, 17], and gives us the value of $D_\infty \simeq 13/5$ [i.e., the same as (18) and (22)].

The closed values of D_∞ were obtained in experiments [18] ([19]) and in the direct numerical simulations of Hosokawa and Yamamoto [20] (see also Discussion).

IV. LOCAL SUBREGIONS OF LARGE GRADIENTS OF PASSIVE SCALAR

Any arbitrary vector field $\mathbf{q}(\mathbf{r})$ can be decomposed into solenoidal part $\mathbf{u}$ and potential part $\nabla\psi$,

$$\mathbf{q} = \mathbf{u} + \nabla\psi.$$

Let us suppose, as in [21], that $\mathbf{u}$ satisfies the equation

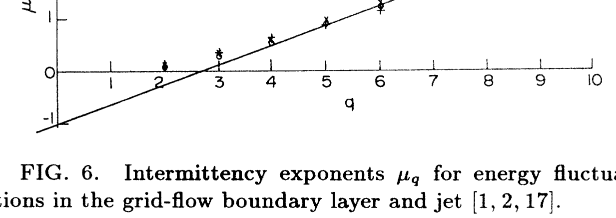

FIG. 6. Intermittency exponents μ_q for energy fluctuations in the grid-flow boundary layer and jet [1, 2, 17].

for the velocity field, while the potential part obeys the following equation:

$$\frac{\mathcal{D}\psi}{\mathcal{D}t} = p/\rho_0 - \mathbf{u}^2/2,$$

where p is a pressure, ρ_0 is a fluid density, and $\mathcal{D}/\mathcal{D}t = \partial/\partial t + (\mathbf{u}\nabla)$. Then for $\mathbf{q}$ we obtain

$$\frac{\mathcal{D}q_i}{\mathcal{D}t} = -q_j\frac{\partial u_j}{\partial x_i} \tag{23}$$

(without a viscous term). Let us describe a passive scalar transfer by the equation

$$\frac{\mathcal{D}c}{\mathcal{D}t} = 0 \tag{24}$$

(without molecular diffusion). Denoting the passive scalar gradients as $\xi_i = \partial c/\partial x_i$, one obtains

$$\frac{\mathcal{D}\xi_i}{\mathcal{D}t} = -\xi_j\frac{\partial u_j}{\partial x_i}. \tag{25}$$

Equation (25) has the same form as (23). Thus in the turbulent flow the subregions with extremely high blips of $\mathbf{q}^2$ coincide with the subregions of ξ_i^2 blips. Hence the scalings of $\mathbf{q}^2$ and $(\nabla c)^2$ in the subregions are governed by the same parameter, α_4 (see Sec. III).

For description of passive scalar transfer in Kolmogorov turbulence the governing parameter $\overline{N} = \langle|\frac{\partial c^2}{\partial t}|\rangle$ (additional to $\bar{\epsilon}$) is used (Sec. 21.6 in [22]), and the spectrum $E_{c^2} \sim \overline{N}\bar{\epsilon}^{-1/3}k^{-5/3}$ is obtained. Then, similarly to the derivation of (18), we estimate the scaling of $(\nabla c)^2$ from dimensional arguments:

$$\max\int_v(\nabla c)^2 dv \sim \overline{N}\alpha_4^{1/5}r^{11/5}, \tag{26}$$

i.e., for the field $(\nabla c)^2$ $D_\infty = 11/5$.

Figure 7 shows μ_q of $(\nabla c)^2$ obtained from experiments [23, 24] and gives us $D_\infty \simeq 11/5$. This value coincides with (26).

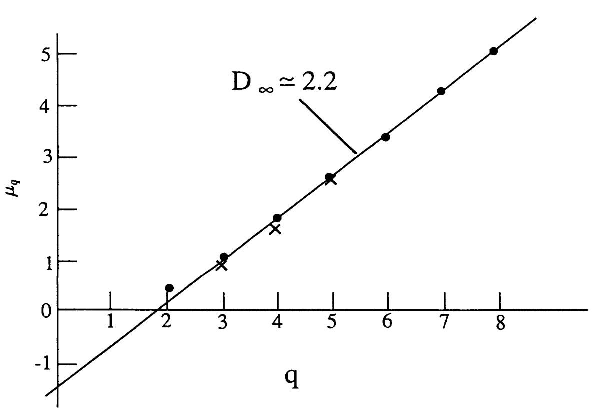

FIG. 7. Intermittency exponents μ_q for passive scalar dissipation $(\nabla c)^2$ in laboratory turbulent flows [23, 24].

V. TURBULENT DIFFUSION IN STABLE STRATIFIED LIQUID

Finally let us discuss the problem of turbulent diffusion in stable stratified fluid (atmospheric and ocean turbulence [22, 25]). It is known that in stable thermostratified media the appearance of large-scale vortices is difficult, because it needs a lot of energy to work against buoyancy forces. Therefore the turbulence exists in the form of internal random waves and spots containing small-scale vortices (Sec. 21.5 [22]).

In a stable stratified media, we can see the following chain of turbulence production: instability of critical shear layer provokes the internal waves [26] and instability of these waves generates spots of small-scale turbulence. The mechanism is similar to the Zaslavsky-Rachko scenario (see Sec. II and [6]), in which the scaling law for diffusivity (K_*) has the form

$$K_* = \frac{1}{6}\frac{d\sigma^2}{dt} \sim \alpha_4^{-1/5}\sigma^{4/5} \tag{27}$$

(σ is the effective scale of the passive scalar spot). Then from (27), we obtain a dispersion law

$$\sigma \sim t^{5/6}. \tag{28}$$

Figure 8 shows the experimental data in a stable stratified atmospheric boundary layer [25, 27]. This figure demonstrates existence of two stages of smoke spot expansion (initial and final). Continuous straight lines present these two stages. The dotted lines show scalings $\sigma \sim t$ and $\sigma \sim t^{3/2}$ (Taylor's and Kolmogorov's dispersion laws). It is seen from Fig. 8 that the initial stage of expansion obeys scaling law (28). This supports the suggestion on small-scale turbulence production in stable stratified flow by collapse of internal waves via the Zaslavsky-Rachko scenario.

VI. DISCUSSION

In the paper the amplitude equations are linked to localized subregions which are not rigidly fixed in the space.

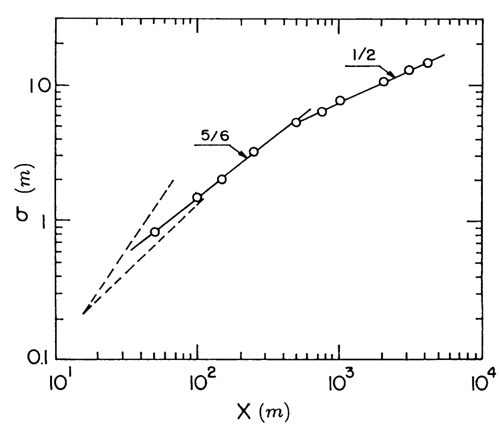

FIG. 8. Dispersion laws for stable stratified atmospheric boundary layer from experiment [27] (circles—experimental data).

For our concrete aim the subregions with Lyapunov index corresponding to Landau cycles can be considered as quasilaminar (i.e., complexity of motion rather than its energy plays the principal role at the *initial* stage). The Zaslavsky-Rachko scenario can then lead to a rapid increase of the complexity of motion and to the energy "blip." There are three types of characteristic time in the problem: (1) the characteristic time of the subregion's (localized traveling waves, solitons, etc.) propagation, τ_p; (2) the characteristic time "inside" of the subregion, τ_i, and (3) the characteristic time (correlation radius) of environment, τ_f. We assume that $\tau_p \geq \tau_i \gg \tau_f$. The first inequality gives us a possibility to use the amplitude approximation and the second one is used in the Fokker-Plank approach. The inequality $\tau_p \geq \tau_i$ is a consequence of self-consistency of the amplitude equation approximation, while the second inequality, $\tau_i \gg \tau_f$, is needed in some *a posteriori* estimations. Indeed, according to our approach the time scale associated with a blip at space scale r is $\tau_i \sim \alpha_4^{1/5} r^{6/5}$. The typical time of the "external" forcing at the same scale can be obtained using the Kolmogorov theory as $\tau_f \sim (\bar{\epsilon})^{-1/3} r^{2/3}$. The required condition, $\tau_i \gg \tau_f$, will be satisfied only if $r \gg \eta_z$, where $\eta_z = (\bar{\epsilon})^{-5/8} \alpha_4^{-3/8}$. Therefore the space scale η_z can be used as a small-scale boundary of the scaling interval in this approach, instead of the Kolmogorov space scale $\eta = (\bar{\epsilon})^{-1/4} \nu^{3/4}$. These scales have different origins, since α_4 governs the balance between stretching of the trajectories and effective diffusion in *phase space* of the Zaslavsky attractor. In the Kolmogorov approach η should tend to zero with $\nu \to 0$. We do not know the behavior of the scale η_z with $\nu \to 0$, but this limit is not a crucial point for our approach, unlike the Kolmogorov one, because of the transitional type of turbulence in the abrupt blip events.

The same reason makes the problem of theoretical definition of the local ("blip") Reynolds number very difficult, because its self-consistency and parameter α_4 seem to be more relevant as a "critical" parameter than molecular viscosity (or Reynolds number) in this case. We have just seen above that this parameter replaces the ν at definition of the small-scale boundary of the scaling interval. Also we cannot use the Kolmogorov estimation $|\alpha_k|^2 \sim k^{-5/3}$ for the remaining Fourier modes if we try to estimate whether the assumptions leading to Zaslavsky mapping are satisfied by the "transitional" turbulence in local "blip." Therefore we can use only the experimental evidence (such as multifractal asymptotics, see above) for justification of this approach. A useful example of concrete work with the Zaslavsky attractor in the terms of the Fokker-Plank equation and demonstration of a bimodal (after averaging over the phases) probability density function can be found in papers [8, 9].

Finally, one can use the Meneveau equation [18] which connects the generalized dimensions for kinetic energy (D_q) with the energy dissipation rate (D'_q),

$$D_q = D'_{2q/3} + \frac{q}{3(q-1)}(D'_{2/3} - D'_{2q/3}),$$

for estimation of D_∞:

$$D_\infty = \frac{D'_{2/3} + 2D'_\infty}{3}.$$

A local anisotropy of real turbulence is the reason for variability of D'_∞. It is shown in [14] that $7/3 \leq D'_\infty \leq 5/2$. If we take $D'_{2/3} \simeq 2.9$ [28] then we obtain $5/2 \leq D_\infty \leq 8/3$. Moreover, since $D'_{2/3} \leq 3$ the value $D_\infty = 13/5$ leads to $2.4 \leq D'_\infty$. Thus one can conclude (in the framework of the Meneveau approach [18]) that physical processes in the local subregions with a large turbulent energy fluctuations can restrict types of instabilities in the subregions with a large rate of energy dissipation [14]. This problem seems to be a very interesting theme for future investigations.

ACKNOWLEDGMENTS

The authors are grateful to E. Kit, I. Hosokawa, C. Meneveau, T. Sanada, K.R. Sreenivasan, A. Tsinober, N. Tsitberlit, K. Yamamoto, and G.M. Zaslavsky for useful information and stimulating remarks. The work was in part supported by Wolfson and Gordon Foundations as well as by the Israeli Ministry of Absorption.

[1] A. Tsinober, E. Kit, and T. Dracos, J. Fluid Mech. **242**, 169 (1992).

[2] A. Bershadskii, E. Kit, A. Tsinober, and H. Vaisburd, Fluid Dyn. Res. **14**, 71 (1994).

[3] L.D. Landau and E.M. Lifshits, *Fluid Mechanics* (Pergamon Press, Oxford, 1959).

[4] G. Nicolis and J.W. Turner, Ann. N.Y. Acad. Sci. **316**, 251 (1979).

[5] A. Bershadskii, E. Kit, and A. Tsinober, Proc. R. Soc. London, Ser. A **441**, 147 (1993).

[6] G.M. Zaslavsky and Kh.-R. Rachko, Zh. Eksp. Teor. Fiz. **76**, 2052 (1979) [Sov. Phys. JETP **49**, 1039 (1979).

[7] G.M. Zaslavsky, Phys. Lett. **69A**, 145 (1978).

[8] K.Y. Tsang and M.A. Lieberman, Phys. Lett. **103A**, 175 (1984).

[9] K.Y. Tsang and M.A. Lieberman, Physica D **11**, 147 (1984).

[10] P. Grassberger and I. Procaccia, Physica D **13**, 34 (1984).

[11] R.V. Jensen and C.R. Oberman, Physica D **4**, 183 (1982).

[12] O.F. Vlasova and G.M. Zaslavsky, Phys. Lett. **105A**, 1 (1984).

[13] G.K. Batchelor, *The Theory of Homogeneous Turbulence* (Cambridge University Press, Cambridge, England, 1953).

[14] A. Bershadskii and A. Tsinober, Phys. Rev. E **48**, 282 (1993).

[15] A. Bershadskii and A. Tsinober, Phys. Lett. A **165**, 37 (1992).

[16] K.R. Sreenivasan, Annu. Rev. Fluid Mech. **23**, 539 (1991).
[17] E. Kit, T. Dracos, and A. Tsinober, in *Proceedings of the Fourth European Conference on Turbulence*, edited by F. Nieuwstadt (Kluwer, Netherlands, 1993).
[18] C. Meneveau, J. Fluid Mech. **232**, 469 (1991).
[19] C. Meneveau and K.R. Sreenivasan, J. Fluid Mech. **224**, 429 (1991).
[20] I. Hosokawa and K. Yamamoto (private communication); see also Phys. Fluids **2**, 889 (1990); J. Phys. Soc. Jpn. **58**, 20 (1989).
[21] G.A. Kuz'min, Phys. Lett. **96A**, 88 (1983).
[22] A.S. Monin and A.M. Yaglom, *Statistical Fluid Mechanics* (MIT Press, Cambridge, MA, 1975), Vol. 2.
[23] K.R. Sreenivasan and R.R. Prasad, Physica D **38**, 322 (1989).
[24] R.A. Antonia and K.R. Sreenivasan, Phys. Fluids **20**, 1800 (1977).
[25] F. Pasquil and F.B. Smith, *Atmospheric Diffusion* (Ellis Horwood, London, 1983).
[26] S.M. Churilov and I.G. Shukman, J. Fluid Mech. **180**, 1 (1987).
[27] V. Högstrom, Tellus **16**, 205 (1964).
[28] S.I. Vainshtein, Y. Du, and K.R. Sreenivasan, Phys. Rev. E **49**, 2521 (1994).

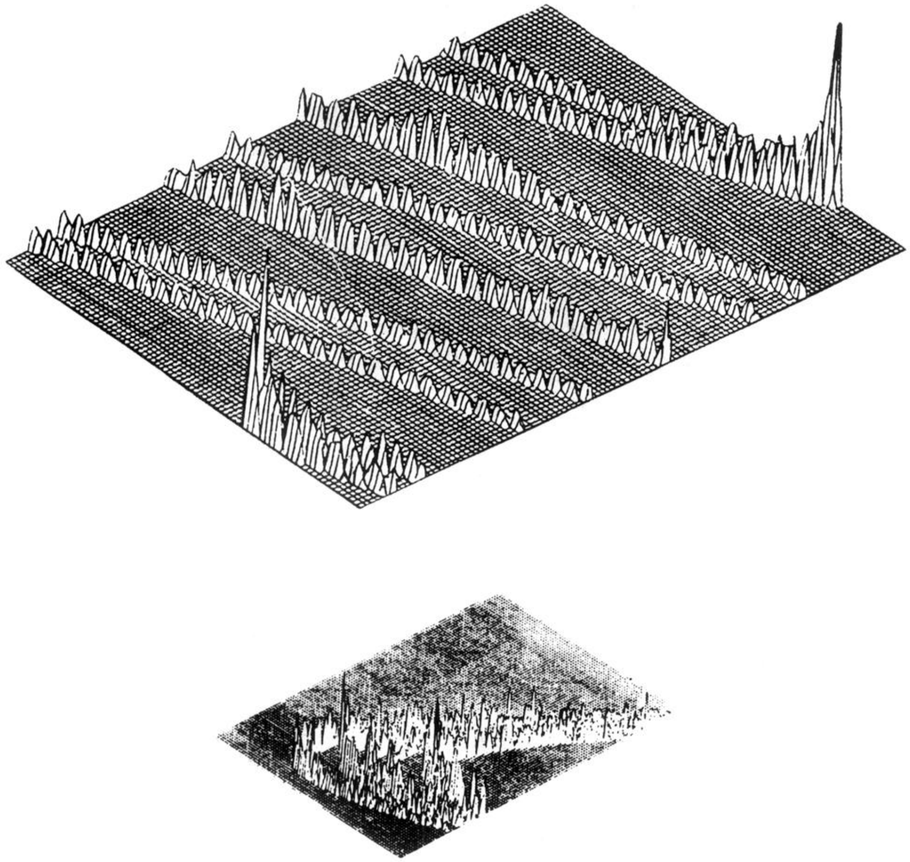

FIG. 4. Distribution function $\rho(x, y)$ on the strange attractor depicted in Fig. 3 [on bottom: the subdivision of the $\rho(x, y)$ in the vicinity of point B].